Coupling detailed urban energy and water budgets with TEB-Hydro model: Towards an assessment tool for nature based solution performances

Xenia Stavropulos-Laffaille, Katia Chancibault, Hervé Andrieu, Aude Lemonsu, Isabelle Calmet, Pascal Keravec, Valéry Masson

Urban Climate 39 (2021) 100925

Contents lists available at ScienceDirect

Urban Climate

journal homepage: www.elsevier.com/locate/uclim

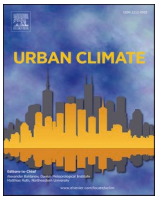

Coupling detailed urban energy and water budgets with TEB-Hydro model: Towards an assessment tool for nature based solution performances

Xenia Stavropulos-Laffaille [a], Katia Chancibault [a,*], Hervé Andrieu [a], Aude Lemonsu [b], Isabelle Calmet [c], Pascal Keravec [c], Valéry Masson [b]

[a] Université Gustave Eiffel, GERS, EE, Campus Nantes, 44344 Bouguenais, France
[b] CNRM UMR 3589, Météo-France/CNRS, Toulouse, 31057 Toulouse, CEDEX 1, France
[c] ECN, LHEEA, 44321 Nantes, Cedex 3, France

ARTICLE INFO

Keywords:
Hydro-microclimate model
Urban microclimate
Urban hydrology
Urban energy - water budgets
Pin Sec catchment

ABSTRACT

Nature-based solutions (NBS) are increasingly promoted to mitigate urbanization effects, such as the urban heat island. The release of latent heat requires the availability of water in the urban soils. Models able to represent both detailed water and energy budgets are needed for a reliable evaluation of NBSs performances. The TEB-Hydro model is a recent hydro-microclimate model that extends the physics of the urban microclimate model TEB-Veg to water processes in urban subsoil in order to represent more realistically coupled water and energy budgets. Hence, the aim of this paper is to evaluate the TEB-Hydro model regarding how the water processes affect the energy balance. The model is applied to an urban French catchment for which both hydrological and microclimate data are continuously collected. The model shows general good performances in both simulating latent and sensible heat fluxes. Nevertheless, soil water contents are slightly underestimated during wet periods and overestimated during dry periods. Compared to the previous version of the model (TEB-Veg) with a simplified water budget, TEB-Hydro tends to more overestimate latent heat fluxes than TEB-Veg during dry periods. During wet periods, however, TEB-Hydro simulates better sensible heat fluxes and latent heat fluxes.

1. Introduction

The water and energy budget of urban areas are both affected by land use and subsurface changes induced by the urbanization process which concern all countries. The use of impervious materials on the one hand increases surface runoff and limits infiltration leading to more frequent and more intense floods, weaker groundwater recharge and urban river base flow (Fletcher et al., 2013; O'Driscoll et al., 2010). On the other hand, artificial materials and urban compactness favour the urban heat island phenomenon by trapping radiation and storing energy during the day and releasing it at night (Grimmond, 2007; Oke, 1987). The mitigation of these damaging consequences of urbanization effects relies the more and more on soil related changes, the integration of vegetation and urban sensitive landscape design (Golden and Hoghooghi, 2018). Thus Nature-based solutions (hereafter NBSs) or also referred to as urban green and blue infrastructures are often promoted to improve life quality, socio-economic and environmental health of cities

* Corresponding author at: Université Gustave Eiffel, Campus Nantes, Allée des Ponts et Chaussées - CS5004, 44344 Bouguenais, Cedex, France.
E-mail address: katia.chancibault@univ-eiffel.fr (K. Chancibault).

https://doi.org/10.1016/j.uclim.2021.100925
Received 5 March 2021; Received in revised form 21 May 2021; Accepted 13 July 2021
Available online 24 July 2021

List of symbols

Q^*	net all-wave radiation (W m^{-2})
Q_F	anthropogenic heat flux (W m^{-2})
H	sensible heat flux (W m^{-2})
LE	latent heat flux (W m^{-2})
ΔS	heat flux storage (W m^{-2})
ΔA	net advection heat flux (W m^{-2})
S	ground heat flux (W m^{-2})
P	total precipitation (kg m^{-2} s^{-1})
Ir	water generated from anthropogenic activities (irrigation) (kg m^{-2} s^{-1})
E_*	evapotranspiration over * compartment (kg m^{-2} s^{-1})
R	runoff (kg m^{-2} s^{-1})
D_*	deep drainage or deep percolation over * compartment (kg m^{-2} s^{-1})
ΔW	variation in water storage both on the surface and in the ground during the simulation period (kg m^{-2} s^{-1})
L_v	latent heat of vaporisation (J kg^{-1})
T_*	water flow by transfer
W_*^{surf}	surface retention capacity over * compartment (mm)
$W_{max,*}^{surf}$	maximum surface retention capacity over * compartment (mm)
I_*	surface water infiltration rate of * compartment (m s^{-1})
R_*^{surf}	surface runoff connected to the sewer network for * compartment (mm s^{-1})
f_{con}	effective connected impervious area fraction (−)
W_*^{gr}	soil moisture content over * compartment (m^3 m^{-3})
t	time step (s)
nb	number of time steps (−)
I_p	parameter representing the water tightness of the sewer pipe (−)
k_{sew}	hydraulic conductivity of the soil (m s^{-1})
D_{sew}	sewer density within a single grid cell (−), expressed by the ratio of the total sewer length in one grid cell (m) to the maximum total sewer length in a single grid cell of the entire study site (m)
C_{rech}	coefficient of recharge (−) in order to limit deep drainage
Q	sewer discharge from ground water infiltration (m^3 h^{-1})
$Q_{*,t}$	discharge at time step t (m^3 h^{-1})
Q_{obs}'	arithmetic mean of observed discharges (m^3 h^{-1})
$F_{*,t}$	heat flux at time step t (W m^{-2})

*Subscripts**

rf	roof
rd	road
gdn	garden
con	connection
veg	vegetation
gr	bare ground surface
sew	sewer
rech	recharge
max	maximum
sim	simulation
obs	observation
v	vertical
h	horizontal

*Superscripts**

gr	ground
surf	surface

(Emmanuel and Loconsole, 2015; Matthews et al., 2015; Norton et al., 2015; Kabisch et al., 2017). Concerning resilient water management, NBSs are based on source control infiltration or water storage representing very often vegetated areas (Lafortezza et al., 2018; Berland et al., 2017; Hamel et al., 2013). City greening is also considered as one of the most important measures for cooling (Hesslerová et al., 2021). Besides solar radiation interception, it reduces urban heat by the release of latent heat flux, in other words by evapotranspiration. Implemented at different spatial scales (green belts, urban parks, alleys, green roofs and walls), the cooling potential of urban vegetation depends on various factors (vegetation species, locations, water availability in the ground, atmospheric

demand, etc.) (Daniel et al., 2018). Nonetheless, Hesslerová et al. (2021) state that "the principals of the cooling potential of vegetation are still misunderstood". Consequently, it is of primary importance to progress towards a better understanding and modelling of NBSs and their influence on both hydrological and energetic processes such as evapotranspiration in urban areas (Mitchell et al., 2008).

Nevertheless, urban hydrological models and urban climate models do not address the evapotranspiration process in the same way. In many urban hydrological models, evapotranspiration is derived from a reference value (i.e. potential evapotranspiration) linked to vegetation type and groundwater availability (DHI, 2012; Grimmond and Oke, 1991; Locatelli et al., 2017; Rodriguez et al., 2005). Berthier et al. (2006) pointed significant differences between two evaporation schemes, detailing soil processes and atmosphere processes respectively. Several recent studies confirmed that the various approaches used to estimate evapotranspiration in urban areas reach different conclusions, and that this subject remains a scientific problem (Litvak et al., 2017; Liu et al., 2017; DiGiovanni-White et al., 2018; Coccolo et al., 2018). As an example, the atmospheric demand is not yet often considered on the local scale and there is no local retroaction from the water to the energy budget. This is however important as DiGiovanni-White et al. (2018) confirm the influence of micrometeorological conditions on evapotranspiration in urban heterogeneous environments. For their part, urban climate models resolve in a very detailed way energy and radiative budgets, while water interactions are simplified, leading to less well modelled latent heat fluxes compared to other fluxes (Grimmond et al., 2011, 2010). Many of those existing urban canopy models coupled with mesoscale models for climate assessment of neighbourhood-scale have been adapted to represent urban vegetation, including trees (Krayenhoff et al., 2014, 2015, 2020; Lee and Park, 2008; Redon et al., 2017, 2020; Ryu et al., 2016). In general, they allow tackling multiple energy and radiation processes between the urban three-dimensional environment and the vegetation (radiation interactions, wind profile modification within the canyon, or trees transpiration). However, they dispose of basic description of water processes and model evaluation is concentrated on the energy budget. For instance, the water availability in soils is not always taken into account (Gros et al., 2016; Nice et al., 2018) which may result in an overestimation of the effect of greening solutions on the urban heat island, during strong heat or dry periods.

Models resolving in a coupled way both water and energy budgets, linked by the evapotranspiration processes, are then required to improve the understanding and to better estimate evapotranspiration in urban areas. In order to reach this objective, hydrological processes together with NBSs, such as urban vegetation, green roofs and trees, are being introduced within the Town Energy Balance (TEB) urban canopy model (Masson, 2000; Lemonsu et al., 2007; de Munck et al., 2013; Lemonsu et al., 2012; Redon et al., 2017, 2020)

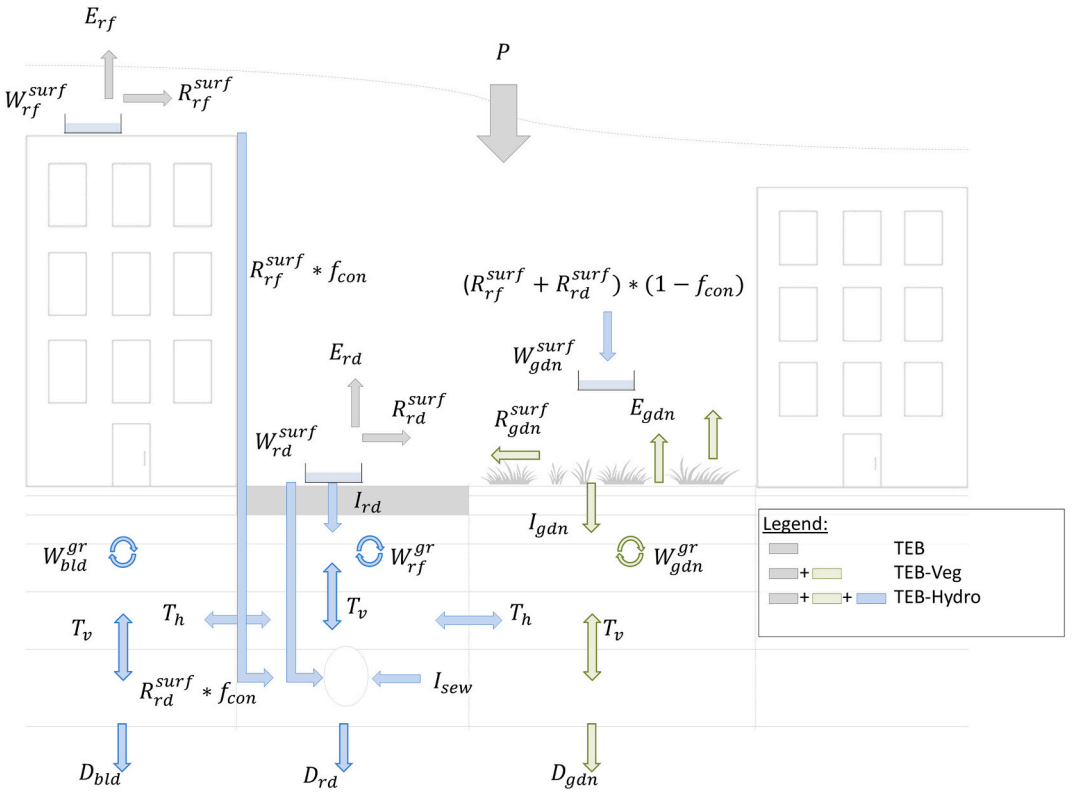

Fig. 1. Schematic view of the different hydrological processes of TEB, TEB-Veg and TEB-Hydro. Inside one grid mesh, horizontal double arrows stand for lateral water flow (T_h) between each soil layer of the compartments and vertical double arrows for vertical water flow (T_v) between each soil layer inside each compartment. ***P*** stands for precipitation, ***E*** * for evaporation, ***R*** * * for runoff, ***I*** * for Infiltration, ***W*** * * for water storage, ***D*** * for deep drainage and f_{con} for effective connected impervious area fraction. Subscripts rd, rf and gdn stand respectively for "road", "roof" and "garden" compartments. Superscripts surf and gr stand respectively for "surface" and "ground" (Stavropulos-Laffaille et al., 2018). The number of ground layers is only indicative. All signs can be found in Appendix A.

that resolves detailed energy and radiative budgets of all urban surfaces (buildings, roads and vegetated surfaces). A canyon approach for a simplified urban morphology is used. A detailed energy budget of green infrastructures is resolved for the soil-vegetation continuum in radiative and energetic interactions with local built-up environment, thanks to the Interaction Soil-Vegetation Biosphere-Atmosphere (ISBA) Transfer model (Boone et al., 1999; Decharme et al., 2011) coupled to the TEB model (Redon et al., 2017, 2020). ISBA also resolves a detailed water budget but initially for the natural compartment only. Stavropulos-Laffaille et al. (2018)- extended it to the one of buildings and roads by introducing in TEB the main hydrological processes specific to urban areas (i.e. weak infiltration through road surfaces and sewer drainage network taken into account). That way, a more elaborated and integrative water budget, influencing evapotranspiration processes, is now available. In summary, the nowcalled model TEB-Hydro is an original hydro-microclimate urban model coupling detailed water and energy processes and operating at the catchment or city scale. It simulates the response of an urban area to time series of atmospheric forcing, including the following hydrological processes: total flow and contributions of each surface type, base flow of the sewer drainage network, total and surface type related evaporation. Nevertheless, the feedback of this new water budget on the energy budget has not yet been studied.

The aim of this study is thus to complete the model evaluation by discussing more precisely the interactions between both water and energy budgets. Therefore, the hydro-microclimate model TEB-Hydro is applied to an experimental catchment (watershed) for which time series of hydrological and meteorological measurements are available. The assessment focuses on the sensible heat flux and the latent heat flux, or evapotranspiration, which couples the water and energy budgets and which presents an important part of the annual water budget. It should be noted that the assessment of modelled evapotranspiration by comparison with field data is not yet frequent, as evapotranspiration rates in heterogeneous urban areas are difficult to measure (DiGiovanni-White et al., 2018).

First, the main terms of both water and energy budgets of TEB-Hydro are described in Section 2. The study site and experimental data are presented in Section 3. Section 4 deals with the simulation configuration of TEB-Hydro and TEB-Veg and introduces the evaluation criteria. In Section 5, the results of TEB-Hydro are first compared to observations and then to the results of TEB-Veg followed by a discussion. A conclusive section ends the paper.

2. The hydro-microclimate model – TEB-Hydro

The model developments are presented in detail in Stavropulos-Laffaille et al. (2018) (Fig. 1). TEB-Hydro can be run in a 2D-coupled way with meteorological models as well as in an offline configuration using observed atmospheric data forcing. It runs with a regular grid mesh with horizontal resolution usually larger than a few hundred meters. Town geometry is simplified thanks to the canyon approach that implies averaging urban cover characteristics and morphology (building height, construction materials, canyon aspect ratio, and street orientation) inside one mesh. The urban vegetation is included inside the canyon, based on Lemonsu et al. (2012). The following presentation is limited to the model equations acting on the energy fluxes and the energy budget.

Detailed radiative and energy budgets are computed over four surface types, representative of three compartments, hereafter called “buildings” (roofs, walls), “roads” and “gardens” (vegetation surfaces and bare soil), fully described in Lemonsu et al. (2012) and Masson (2000). TEB computes an average surface temperature for each surface type according to net solar and infrared radiation (Q^*), sensible (H) and latent (LE) heat fluxes and conduction heat fluxes. The conduction heat fluxes are calculated between different material layers discretising each surface type. The net radiation (or net energy absorbed) is calculated by taking into account the multiple inter-reflections of solar and infrared radiation between all canyons’ facets.

Therefore, the integrative energy budget of the urban canopy layer can be expressed as:

$$Q^* + Q_F = H + LE + \Delta S + \Delta A \left[W \cdot m^{-2}\right] \tag{1}$$

with Q_F the anthropogenic heat flux, ΔS the heat flux storage resulting from heat conduction in urban infrastructures and in the soil, and ΔA the net advective heat flux.

The water budget of the urban canopy layer is expressed as:

$$P + Ir = E + R + D + \frac{\Delta W}{\Delta t} \left[kg \cdot m^{-2} \cdot s^{-1}\right] \tag{2}$$

with P the total precipitation, Ir the water flux generated from anthropogenic activities (irrigation), E the evapotranspiration, R the total runoff, D the deep drainage (also referred to as deep percolation), ΔW the variation in water storage both on the surface and in the subsoil during the simulation period (Δt).

Both budgets are coupled through the mechanism of water vapour exchange between soil and vegetation and the atmosphere:

$$LE = E \times L_v \left[W \cdot m^{-2}\right] \tag{3}$$

with L_v the latent heat of vaporisation ($J \cdot kg^{-1}$).

For horizontal built-up surfaces, water coming from precipitation and irrigation, which does not runoff directly into the urban water system, is intercepted at the surface and evaporates as turbulent latent heat flux (LE). This flux is conditioned by the available water in the surface water interception reservoir, and its intensity depends on the surface specific humidity at saturation, air humidity (inside the canyon for roads and above the canopy level for roofs), and turbulent exchange coefficients varying with wind speed and surface roughness length. The total amount of water evaporated by the gardens (E_{gdn}), combines the following contributions of vegetation evapotranspiration (E_{veg}) and evaporation from the ground (E_{gr}) (Lemonsu et al., 2012):

$$E_{gdn} = E_{veg} + E_{gr} \left[kg \cdot m^{-2} \cdot s^{-1}\right] \quad (4)$$

The water content evolution of the interception water reservoir of each surface type is impacted by rainfall and evapotranspiration (Masson, 2000):

$$\frac{\partial W_{*}^{surf}}{\partial t} = P - E_{*} - I_{*} \left[kg \cdot m^{-2} \cdot s^{-1}\right] \quad (5)$$

where * stands for roof, vegetation or bare ground and I_* (m.s^{-1}) stands for water infiltration ($I_{rf} = 0$).

When W_{*}^{surf}(m) exceeds the maximal reservoir capacity ($W_{*,max}^{surf}$), surface runoff is produced. It is collected by stormwater or combined sewer networks according to the connected fraction (f_{con}) of impervious areas (Sutherland, 2000).

The water stored in the soil is important since evapotranspiration depends directly on this water amount. The water and energy exchanges in the subsoil of buildings, roads, and gardens are computed in order to calculate the temporal evolution of soil water contents and soil temperatures. Sewer networks drain ground water when the water table rises above the sewer trenches level (Belhadj et al., 1995; Berthier et al., 2004; Rodriguez et al., 2020). The infiltration into the sewer network, denoted I_{sew} (m.s^{-1}) is expressed as follows:

$$I_{sew} = k_{sew} \times I_p \times D_{sew} \left[m \cdot s^{-1}\right] \quad (6)$$

with k_{sew} (m.s^{-1}) the hydraulic conductivity of the soil layer where the sewer is situated, I_p (−) the parameter that describes the state of watertightness of the sewer pipe, D_{sew}(−) the sewer density in the grid mesh.

In order to favour ground water infiltration into the sewer network during wet periods, the deep drainage (i.e. low boundary condition of the model soil compartment for water flux) is partially or totally retained, according to a coefficient of recharge C_{rech}, (detailed in Stavropulos-Laffaille et al. (2018)). Moreover, lateral water transfer between each compartment is performed by taking

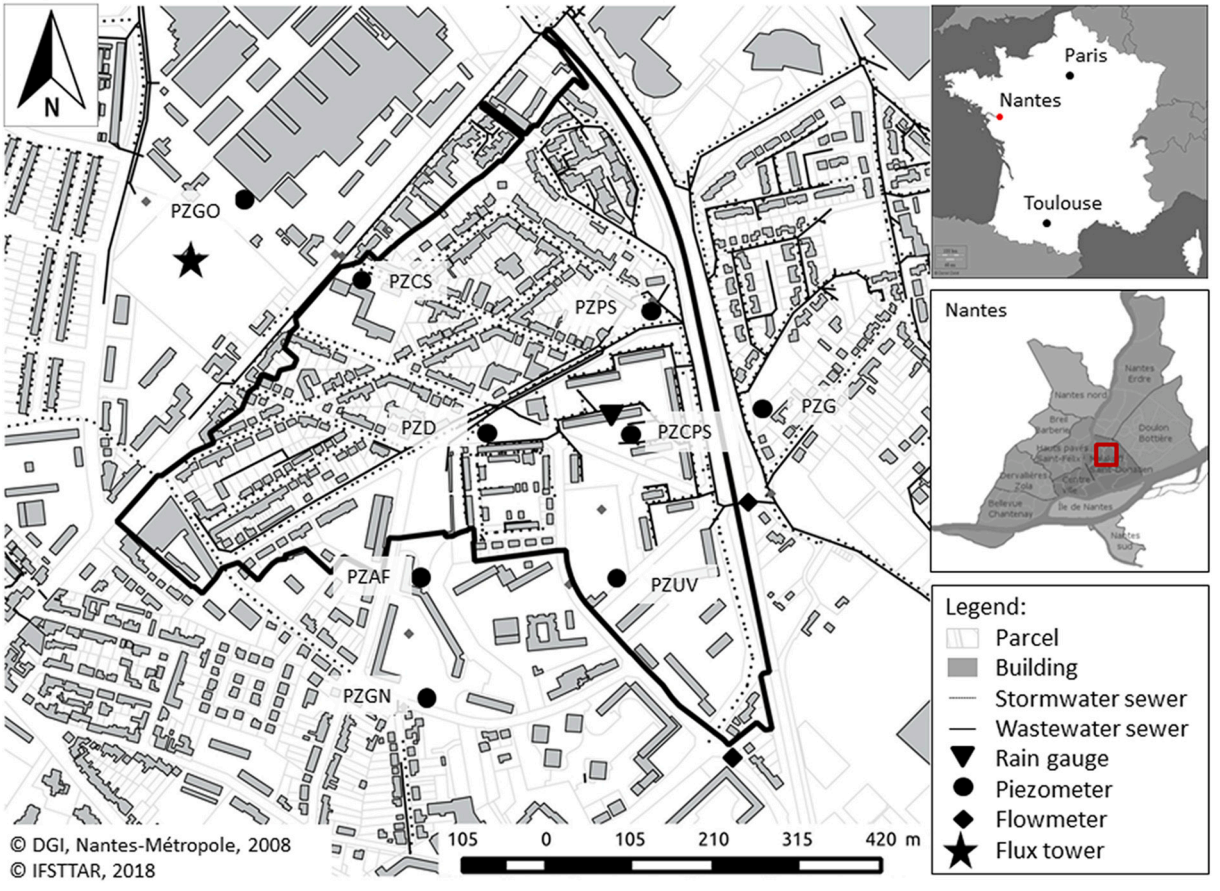

Fig. 2. Limits of the urban catchment Pin Sec (thick black line). Black thin line: storm water sewer network, black thick line: waste water sewer network, points: piezometers, triangles: rain gauge, diamonds: flowmeter. The maps on the right side of the catchment indicate the location of Nantes, in France (above) and of the Pin Sec catchment (red square) in Nantes (middle). (For interpretation of the references to color in this figure legend, the reader is referred to the web version of this article.)

into account a soil water content exponential decay, tending towards the mean water content of all three compartments, which is limited by the soil water content at its wilting point.

As a result, the water budget of each compartment (road, roof and garden respectively) is described as follows:

$$E_{rd} + I_{sew} + D_{rd} + R_{rd}^{surf} = P + \left(\Delta W_{rd}^{gr} + \Delta W_{rd}^{surf}\right) \times \frac{1}{\Delta t} \tag{7}$$

$$E_{rf} + R_{tf}^{surf} + D_{rf} = P \tag{8}$$

$$E_{gdn} + D_{gdn} + R_{gdn}^{surf} = P + \left(R_{rf}^{surf} + R_{rd}^{surf}\right) \times (1 - f_{con}) + \left(\Delta W_{gdn}^{gr} + \Delta W_{gdn}^{surf}\right) \times \frac{1}{\Delta t} \tag{9}$$

with D_* and $R_*{}^{surf}$ $(kg \cdot m^{-2} \cdot s^{-1})$, the deep drainage and the surface runoff for each compartment, respectively. $\Delta W_*{}^{gr}$ $(kg \cdot m^{-2})$ is the variation of soil water content of the soil column, $\Delta W_*{}^{surf}(kg \cdot m^{-2})$, the variation of the surface interception reservoir of each surface type, f_{con}(-), the fraction of impervious surfaces connected to the sewer and $(R_{rf}^{surf} + R_{rd}^{surf}) \times (1 - f_{con})$ $(kg \cdot m^{-2} \cdot s^{-1})$, the rate of water reaching the subsoil from artificial surfaces not connected to the sewer network.

TEB-Hydro simulates a total discharge and separated contributions by surface type and from ground water infiltration as well as latent and sensible heat fluxes. Thus, measurements of all of these fluxes are needed for a comprehensive evaluation. The Pin Sec catchment in the city of Nantes, located in the Northwest of France, offers such a database.

3. Case study: the Pin Sec urban catchment

3.1. Characteristics of the study area

The Pin Sec catchment is located in the Eastern part of Nantes, between the Erdre and the Loire Rivers. Nantes is the sixth most populated French city with more than 300,000 inhabitants in 2015 (https://www.insee.fr/fr/statistiques/2011101?geo=COM-44109, consulted in January 2020.). Situated about 40 km from the Atlantic coast, the city has an oceanic climate with mild and rainy winters and fresh summers. The mean annual temperatures range from 8.3 °C to 16.7 °C between 1981 and 2001 (http://www.meteofrance.com/climat/france/nantes/44020001/normales, consulted in January 2020). The mean annual total rainfall is 819.5 mm with frequent but low intensity rains. The catchment, developed between 1930 and 1970, spans over 31 ha. The site is mainly residential including single-family housing with private gardens in the northern part and four-storey multi-family buildings with public parks in the southern part (Fig. 2). The separated sewer network comprises a wastewater and a stormwater sewer.

3.2. Observation data

The catchment has been part of the French observatory ONEVU (Observatoire Nantais de l'EnVironnement Urbain) since 2006, which aims to monitor water and pollutant fluxes and soil-atmosphere exchanges in Nantes urban environment. The site has been instrumented continuously for a decade and has therefore a complete database spanning over a long time period (Mestayer et al., 2011). The following measurements are available (Fig. 2): rainfall, discharges in the storm water and wastewater sewer networks, soil water content, ground water level, turbulent fluxes (latent and sensible heat fluxes), micro-meteorological data (wind speed and direction, air temperature and humidity, atmospheric pressure, incoming solar radiation).

Latent and sensible heat fluxes are measured using the eddy-covariance (EC) method with a setup situated at 26 m above ground level on a lattice tower located on the west border of the catchment. The displacement height and the aerodynamic roughness length of the site are approximated to 8 and 1.2 m respectively (Bagga, 2012). The EC data has been obtained for three years, from 1st of January 2010 to 31st of December 2012. A 3D ultrasonic anemometer (USA-1, Metek GmbH) measured the wind component. The water vapour fluctuations were observed with an open-path infrared gas analyser (LI-7500, LI-COR Biosciences) from 1st of January 2010 to 27th of April 2012 following by a closed-path gas analyser (LI-7200, LI-COR Biosciences) until the end of the period. This flux data needs pre-processing in order to be qualified before comparing with simulated flux data.

The urban data bank of Nantes Métropole provides location of sewer pipes, buildings and informs about their depth, height, length or area.

3.3. Flux data pre-processing

The wind and water vapour data are recorded at a frequency of 20 Hz. The obtained dataset is processed, with additional meteorological data from the closest Météo-France station (situated at Bouguenais airport, 12.3 km away from the measuring mast). Version v6.2.2 of EddyPro® open source software is used to calculate hourly fluxes. Its default settings are applied with the exception of the use of (Ibrom et al., 2007) correction for the low-pass filtering effect. The resulting flux data is then filtered to exclude periods where latent heat is not within an acceptable range (-50 W·m^{-2} to 500 W·m^{-2}). Steady state and developed turbulent conditions tests (Foken et al., 2004) are usually performed. However, in our case, the data is filtered, of which both sensible and latent heat steady state flags are higher than two (i.e. steady test >30%). As stated by Fortuniak et al. (2013), the developed turbulent conditions test does not seem to behave properly in urban areas and would lead to eliminate many acceptable periods. Once these constraints applied, the flux data set is substantially reduced to about 28% for the total simulation period. The main reasons for this poor availability are three major

instrument maintenances. The effect of the filtering lead also leads to many discontinuities in the dataset (Fig. 3 and Fig. 4).

4. Evaluation method of TEB-Hydro

TEB-Hydro simulates various fluxes that contribute to both the water and the energy budgets, coupled by evapotranspiration. As the experimental setting of the Pin Sec catchment gathers both water and energy flux measurements on-site, the evaluation of TEB-Hydro is integral. It can be noticed that this approach is not yet frequently applied, and thus original. Indeed, most of existing model evaluations in hydrology highlight only one type of water flux or stock, respectively the catchment outflow or the groundwater table. This implicitly increases the degrees of freedom in the model parameterisation and assessment. Therefore, thanks to the available data, the TEB-Hydro evaluation is demanding and rigorous. In addition, it includes a comparison between TEB-Hydro and its former version, TEB-Veg. This comparison allows assessing the impact of the newly introduced hydrological parameterisation on the energy part (see Fig. 1). The simulation configurations of TEB-Hydro and TEB-Veg for the Pin-Sec catchment are presented, followed by the definition of the evaluation criteria.

4.1. Simulation configurations of TEB-Hydro and TEB-Veg

Both TEB-Hydro and TEB-Veg simulation configurations are applied to the Pin Sec catchment as done by Stavropulos-Laffaille et al. (2018). As summarised hereafter, the model runs on a single grid mesh (1D). It operates in "off-line" mode, i.e. forced by hourly local meteorological observations (incoming short- and long-wave radiation, pressure, snowfall and rainfall, air temperature and humidity, wind speed). The model's numerical time step is 5 min.

The use of available geographical databases and a GIS allowed estimating different land use and morphological parameters for the model (Table 1). Building and road covers represent respectively 19% and 32%, while vegetated areas (high and low vegetation, bare ground) represent 49% of the total area. The wastewater and storm water sewer networks have a total length of about 7.0 km and 3.9 km respectively, with a mean depth estimated to about 1.5 m below ground. The average weighted height of buildings is about 9.0 m. A detailed survey, conducted by Nantes Métropole in January and March 2014, allowed estimating the ratio of impervious surfaces connected to the stormwater network to 61%. The building materials characteristics are defined based on the buildings' construction period (Table 1). The soil texture at 35 cm below ground is 51% sand, 41% silt and 8% clay. Soil samples were taken at this depth from several soil water content measurement points. The soil is discretised into 12 layers over a total depth of 3 m, with layer thicknesses increasing from 1 mm to 1 m in depth.

For TEB-Hydro, the model calibration is used resulting from Stavropulos-Laffaille et al. (2018). The parameter set is $I_p = 0.09$, $I_{road} = 10^{-5}$ mm.s^{-1} and $C_{rech} = 98\%$ with Kling-Gupta efficiency (KGE) (Gupta et al., 2009) values of 0.82 and 0.62 respectively for each period from 9th of January 2010 to 8th of December 2011 and from 9th of January 2011 to 8th of December 2012. Due to a reduced dataset of observed heat fluxes, the reference simulation period is extended to a three-year period from the 1st of January 2010 to the 31st of December 2012.

The TEB-Veg simulation is performed with a similar configuration (catchment features) to the TEB-Hydro simulation. Only the hydrological module is set inactive, except in the garden compartment, and at the road- and roof-surfaces (Lemonsu et al., 2012). Therefore, the water transfer in the subsoil of both "building" and "road" compartments is no longer considered and the maximal surface interception capacity (also referred to as the potential wetting loss) is fixed to 1 mm for both roof- and road-surfaces. Deep drainage in the "garden" compartment is not limited in this version. Impervious surface runoff is considered to be totally collected by

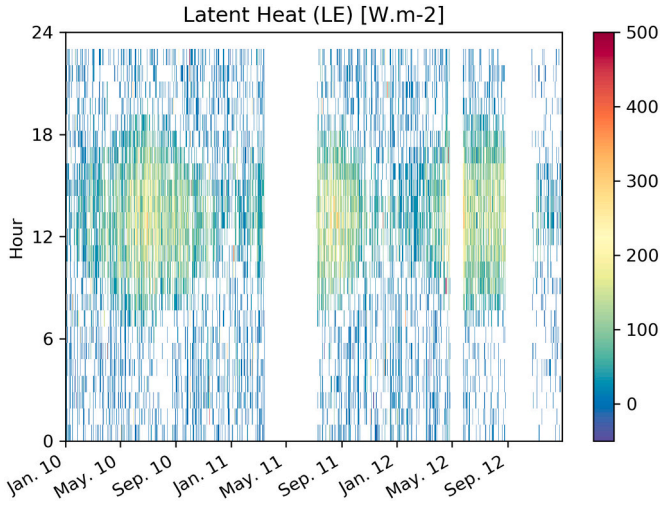

Fig. 3. Heatmap of daily and hourly variations of Latent Heat (LE) calculated by the Eddy Covariance method. Unavailability of valid data is represented by the white color.

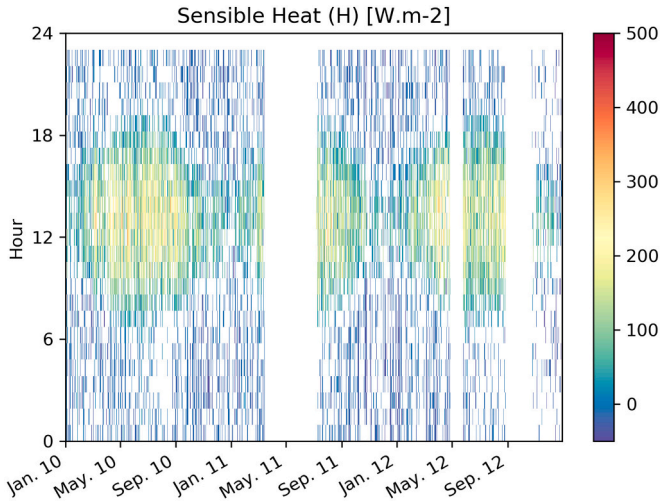

Fig. 4. Heatmap of daily and hourly variations of Sensible Heat (H) calculated by the Eddy Covariance method. Unavailability of valid data is represented by the white color.

Table 1
Land use and morphological parameter values for TEB-Hydro and TEB-Veg simulations on the Pin Sec catchment. The parameters in italic are not used for TEB-Veg simulations.

Urban cover		Building Materials characteristics	
Fractions of buildings	0.19	Principal materials of roofs	Tile
Fractions of roads	0.32	Principal materials of walls	asphalt
Mean building height (m)	9.33	Principal materials of streets	concrete
Roughness length for momentum z0	0.93	Number of road layers	5
Storm water sewer length (m)	*3911.0*	Number of walls and roofs layers	3
Wastewater sewer length (m)	*6972.7*	Soil properties	
Mean sewer depth (m)	*1.5*	Number of soil layers	12
Fractions of imp. Surf. connected to sewer	*0.61*	Fractions of clay	0.08
Natural cover		Fractions of sand	0.51
Fractions of gardens	0.49		

the storm water sewer network, even if it does not exist in a physical way. The subsoil thermal transfers are taken into account in a simpler way, by the mean of a deep ground temperature value.

4.2. Evaluation scores

The simulation performances are evaluated thanks to different scores depending on the variables. For water fluxes, the percent bias PBIAS (%) and the Nash-Sutcliffe efficiency coefficient NSE (−) (Moriasi et al., 2007) are used:

$$PBIAS = \frac{\sum_{t=1}^{nb}\left(Q_{obs,t} - Q_{sim,t}\right)}{\sum_{t=1}^{T} Q_{obs,t}} \times 100 \tag{10}$$

$$NSE = 1 - \frac{\sum_{t=1}^{nb}\left(Q_{sim,t} - Q_{obs,t}\right)^2}{\sum_{t=1}^{nb}\left(Q_{obs,t} - Q_{obs}^{'}\right)^2} \tag{11}$$

with *nb* the number of time steps, $Q_{sim,t}$ and $Q_{obs,t}$, respectively simulated and observed discharges at time step *t*. $Q_{obs}^{'}$ is the arithmetic mean of observed discharges.

For heat fluxes, the root-mean-square-error RMSE ($W{\cdot}m^{-2}$) is used but only calculated on time steps with available observed heat fluxes:

$$RMSE = \sqrt{\frac{\sum_{i=1}^{nb}\left(F_{sim,t} - F_{obs,t}\right)2}{nb}} \tag{12}$$

where $F_{sim,\ t}$ and $F_{obs,\ t}$ are respectively simulated and observed (sensible or latent) heat fluxes at time step t.

In order to evaluate the model's ability to simulate sensible and latent heat fluxes and their seasonal variabilities, daily cycles of simulated and observed hourly heat fluxes are monthly averaged and compared from January 2010 to December 2012.

In the catchment, soil water content measurements at different locations (Fig. 2) are available at a depth of 35 cm from the 1st of May 2010. This 35 cm depth (depth between 20 and 40 cm) corresponds to the sixth soil layer of the model garden compartment. Both observed and simulated ground water are compared.

5. Results

A complementary evaluation of TEB-Hydro to Stavropulos-Laffaille et al. (2018) is performed, based on coupled water and radiative processes. In order to provide a comprehensive interdisciplinary view of the model functioning, its evaluation includes the comparison of modelled to observed values for the following variables: outflow due to ground water drainage, soil water content, sensible and latent heat fluxes simulated by TEB-Hydro. A particular interest is granted to the latent and sensible heat fluxes, which representation is not commonly considered in a hydrological model evaluation. In addition, the comparison of TEB-Hydro to TEB-Veg (Lemonsu et al., 2012) aims to investigate the potential benefits of taking into account new hydrological processes on the models energy budget.

5.1. Comparison of TEB-Hydro to observation data

According to the availability of observed data, the evaluation period of the different variables can differ (Table 2).

5.1.1. Water processes

Stavropulos-Laffaille et al. (2018) performed a first hydrological evaluation of TEB-Hydro, based on a sensitivity analysis and a model calibration on two urban residential catchments. They notably evaluated the model performance on total observed storm water sewer discharges. The findings showed a tendency of TEB-Hydro to consistently overestimate the total storm water sewer discharge as well as to perform better under wet climate conditions. However, they did not address in detail the drainage of soil water by the sewer system. We consider thereafter only observations of the sewer discharge due to soil water infiltration and the soil water content, which are representative of the available soil water for evapotranspiration. This is done, with the aim of discussing more precisely the interactions between both water and energy budgets.

During winter, observations at the Pin Sec catchment show that the groundwater table reaches the sewer network, thus leading to infiltrations into the sewer pipes. A strong correlation has been highlighted between piezometer data of the groundwater table *h (m)* and the base flow inside both stormwater and wastewater networks (Rodriguez et al., 2020) allowing to calculate the contribution of groundwater infiltration to the discharge as following $Qinf = 0.02\ h^2 + 0.74\ h + 7.44$. Compared to observation-based groundwater infiltration discharges, a significant underestimation of simulated values can be highlighted (Fig. 5). Considering the fact that the groundwater table is observed to be below the sewer network during summer, it is very unlikely to observe a base flow due to groundwater infiltration equal to the spring and autumn periods. Moreover, due to a strong sensitivity to the input data depending on the water table, the observation-based groundwater infiltration discharges have to be used cautiously. Therefore, only dynamics of this process are considered, of which TEB-Hydro shows a good reproduction.

In addition, the simulated soil water amplitude compared to observed soil water content is weaker and thus overestimated during dry periods and inversely underestimated during wet periods. Nevertheless, the soil water dynamics in regard to event based variations are well simulated by both models (Fig. 6). If dynamics are satisfying, simulated TEB-Hydro water content amplitudes have been significantly degraded during dry periods. This is related to the different introduced hydrological processes between the urban subsoil of natural and built-up surfaces (horizontal interaction of soil water and deep drainage regulation) (Stavropulos-Laffaille et al., 2018).

5.1.2. Latent and sensible heat fluxes

The assessment of heat fluxes is performed by considering two temporal scales: i) the yearly flux, which intervenes in the budget, ii) the monthly averaged hourly flux which represents both the flux pattern during the day and the evolution of this pattern during a year.

The PBIAS and RMSE scores calculated for TEB-Hydro simulated latent and sensible heat fluxes are shown respectively in Fig. 7 and Fig. 8. The PBIAS is satisfactory for latent heat fluxes (−11.7%) but not for sensible heat fluxes (−41%). RMSE indicates better skills for TEB-Hydro to simulate latent heat fluxes (12.6 $W.m^{-2}$) than sensible heat ones (26.4 $W.m^{-2}$). Distinguishing yearly values, all scores in 2011 highlight a better performance for latent heat fluxes. For sensible heat fluxes, PBIAS is worse in 2011 than in 2010 and 2012. For latent heat fluxes, PBIAS shows less overestimation, except in 2011 when they are slightly positive. The scatter plots of simulated and observed heat fluxes show good results for both simulated LE and H, with respectively a R^2 value of approx. 0.7 and 0.8 (Fig. 9).

The monthly averaged hourly heat fluxes over the 3-year period outline different behaviours of TEB-Hydro, depending on seasons

Table 2
Observed data used for TEB-Hydro evaluation and evaluation period limits.

Observed data	Beginning of evaluation period	End of evaluation period
Outflow of the catchment's sewer network	01/01/2010	31/12/2012
Soil water content	01/05/2010	31/12/2012
Heat fluxes	01/01/2010	31/12/2012

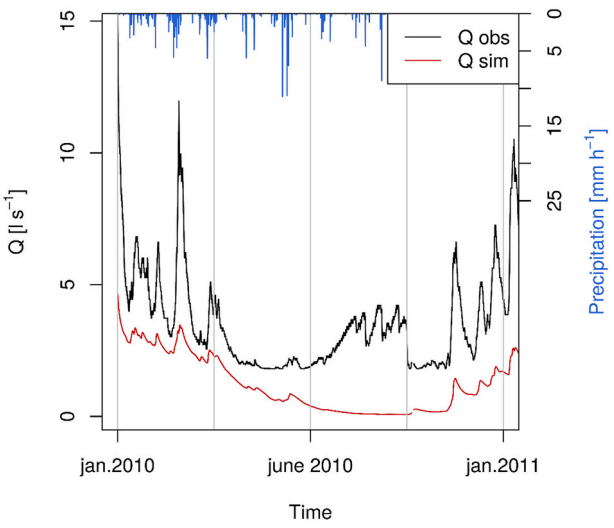

Fig. 5. Simulated (red) discharges from groundwater infiltration by TEB-Hydro during the year 2010, at the Pin Sec catchment. Groundwater infiltration discharges (black) calculated from observed piezometer data (h) during the same period have been calculated from the equation Qinf = $0.02\ h^2 + 0.74\ h + 7.44$ (Rodriguez et al., 2020). (For interpretation of the references to color in this figure legend, the reader is referred to the web version of this article.)

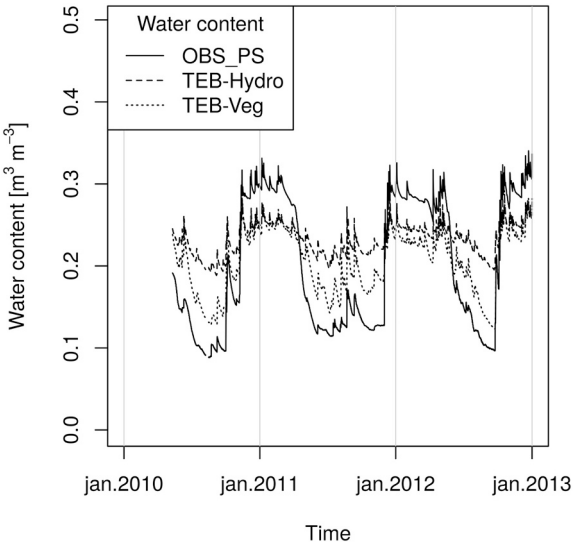

Fig. 6. Observed (black line) and simulated water content by TEB-Hydro (dashed line) and TEB-Veg (dotted line) from May 2010 to December 2012 in the 6th soil layer of the garden compartment, corresponding to a soil depth of 35 cm.

(Fig. 10 and Fig. 11). Regarding autumn and winter, the hourly latent heat fluxes are quite well reproduced by TEB-Hydro. In spring and summer however, they are overestimated. This is coherent with water content simulations. On the contrary, sensible heat fluxes are overestimated in autumn and winter whereas in spring and summer, simulated sensible heat fluxes fit with observed ones. Nevertheless, sensible heat fluxes are overestimated during night-time despite the season.

5.2. *TEB-Hydro and TEB-Veg heat flux comparison*

According to the PBIAS, TEB-Veg compares better to observed latent heat fluxes than TEB-Hydro (respectively 3.1% and − 11.7%) for the whole period. Only in 2011, PBIAS for TEB-Hydro is closer to zero than TEB-Veg's PBIAS (respectively 7.9% and 20.8%) (Fig. 7). RMSE shows slight higher values for TEB-Hydro for the whole period and each single year, (Fig. 8) except in 2011. For sensible heat fluxes, both TEB-Hydro and TEB-Veg obtain very bad PBIAS values (respectively −41% and − 52.2%) (Fig. 7), however RMSE indicates more satisfactory values (respectively 26.4 and 27.9 W.m^{-2}) (Fig. 8). This is probably related to the errors in night-time

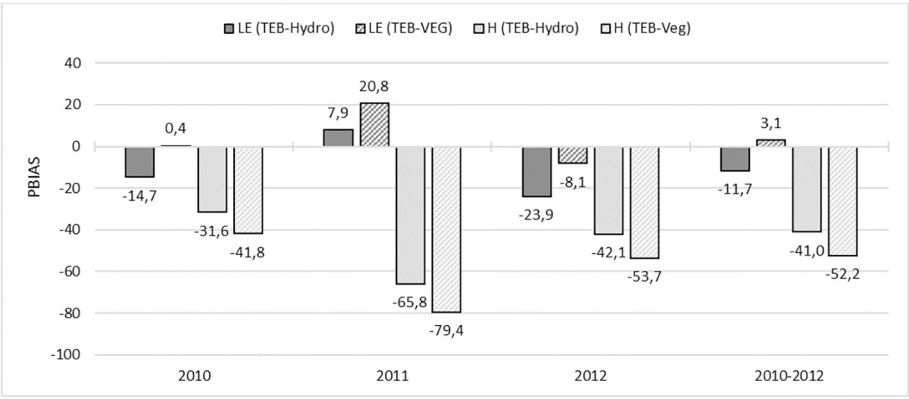

Fig. 7. PBIAS values comparison between simulated and observed latent (dark grey) and sensible (light grey) heat fluxes for TEB-Hydro (full coloured) and TEB-Veg (dashed) configurations. The full period 2010–2012 (right side) and each single year (left side) are detailed.

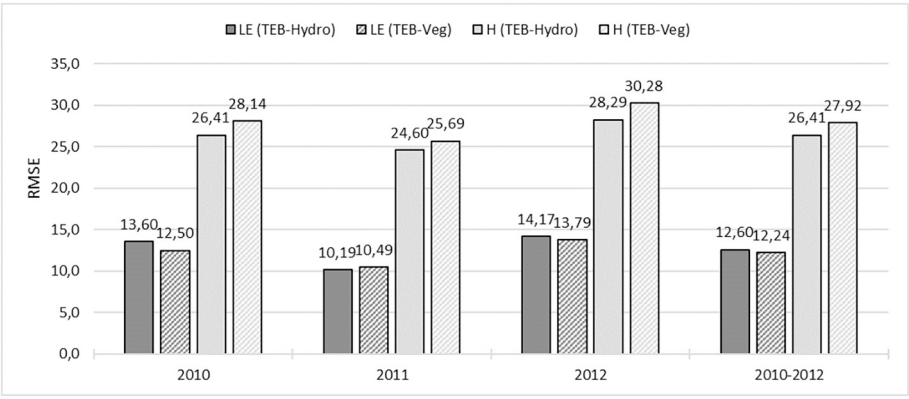

Fig. 8. RMSE values comparison between simulated and observed latent (dark grey) and sensible (light grey) heat fluxes for TEB-Hydro (full coloured) and TEB-Veg (dashed) configurations. The full period 2010–2012 (right side) and each single year (left side) are detailed.

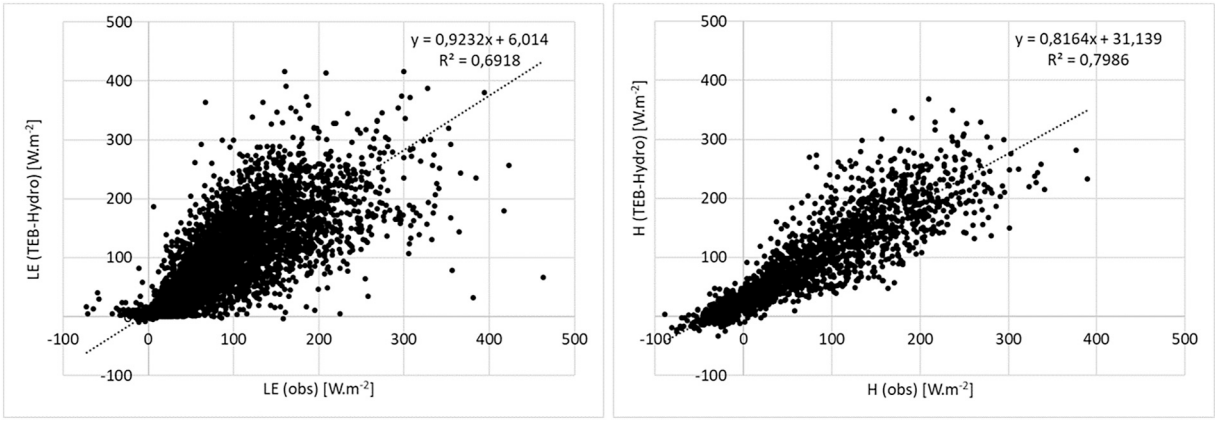

Fig. 9. Scatter plots of TEB-Hydro simulated versus observed latent (LE) and sensible (H) heat fluxes.

simulated fluxes, shown by the monthly average hourly heat fluxes (Fig. 10 and Fig. 11).

The monthly averaged hourly latent heat fluxes show that when TEB-Hydro fits well with observed latent heat fluxes in autumn and winter, TEB-Veg underestimates them (Fig. 10). On the contrary, in spring and summer, simulated TEB-Veg monthly averaged hourly latent heat fluxes are closer to observations, while TEB-Hydro overestimates them. In winter, TEB-Veg monthly averaged hourly sensible heat fluxes are more overestimated than TEB-Hydro ones (Fig. 11). In spring, both TEB-Hydro and TEB-Veg monthly averaged

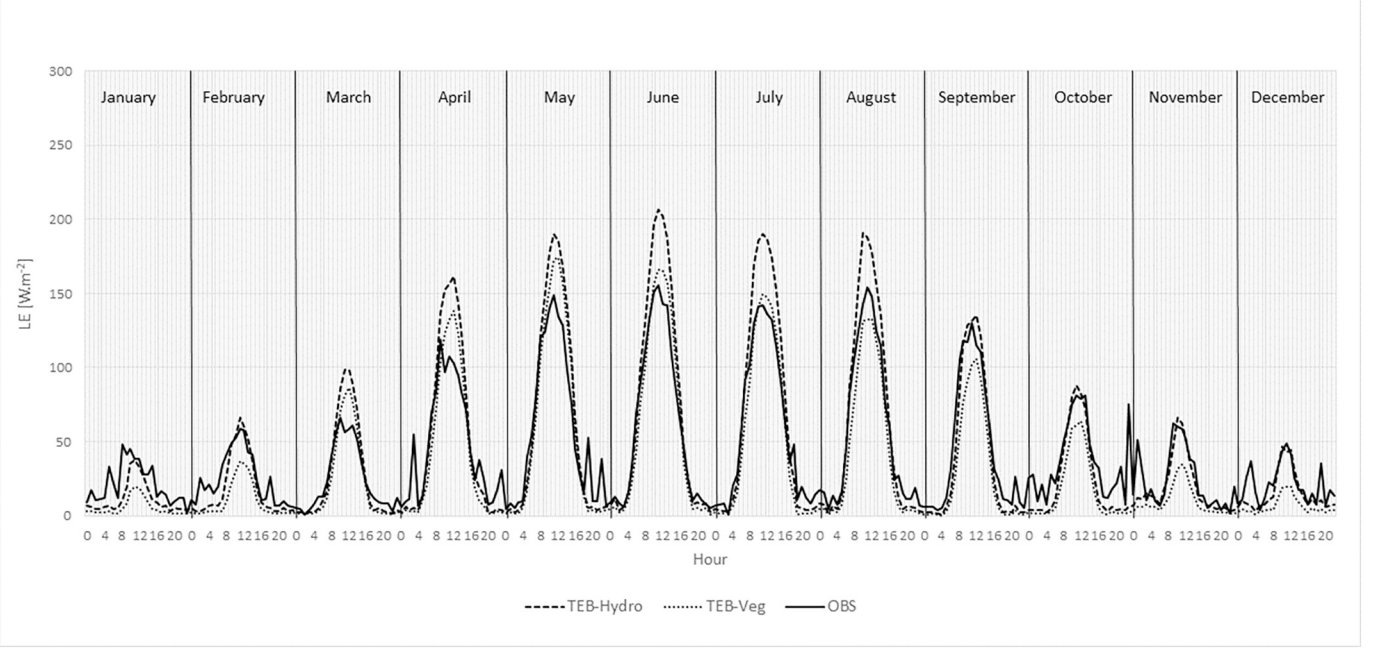

Fig. 10. Monthly averaged hourly latent heat fluxes, over the 3-year period, simulated by TEB-Hydro (dashed line) and TEB-Veg (dotted line) compared to the observed ones (black line).

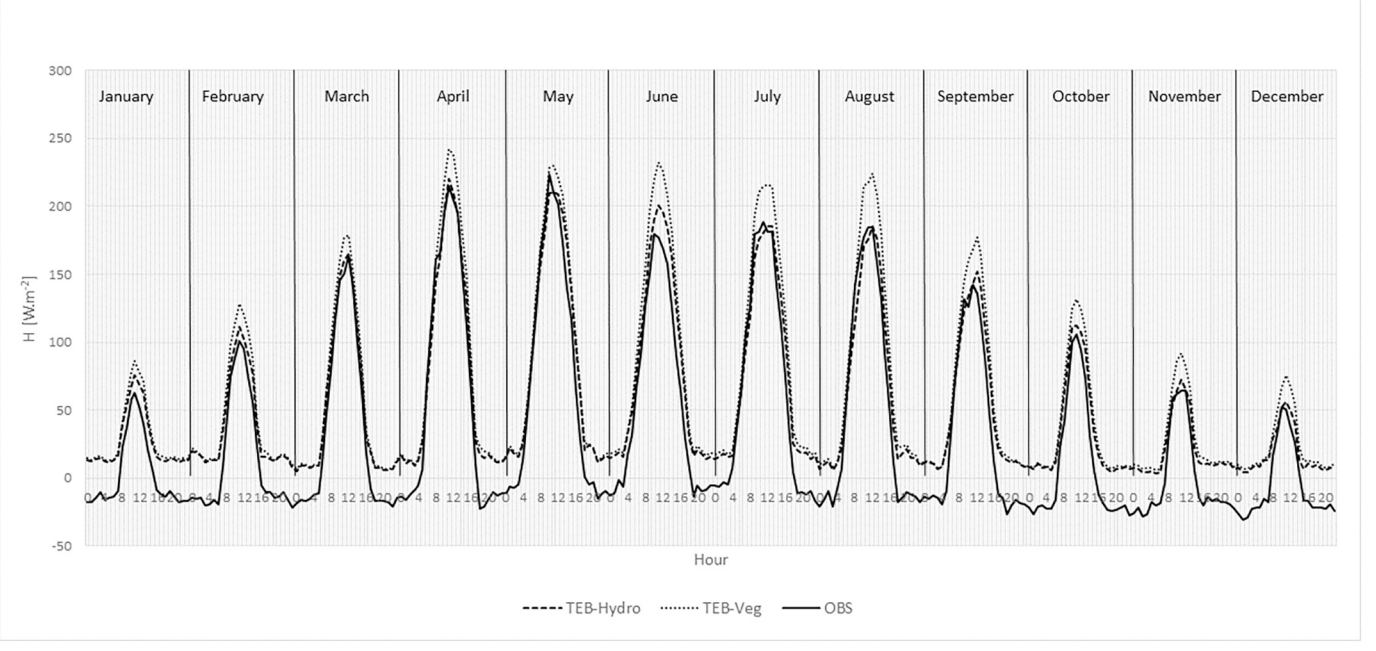

Fig. 11. Monthly averaged hourly sensible heat fluxes simulated by TEB-Hydro (dashed line) and TEB-Veg (dotted line) compared to the observed ones (black line), over the 3-year period.

hourly sensible heat fluxes fit to observed ones. A comparison of all simulated averaged hourly heat fluxes between 2010 and 2012 (sensible and latent heat flux and heat flux storage) between TEB-Hydro and TEB-Veg shows a similar heat flux storage for both models (Fig. 12 and Fig. 13). Therefore, it can be noted for further discussion that differences in both hourly energy budgets are only derived from sensible and latent heat.

In addition, a comparison of all observed and simulated monthly averaged Bowen-ratios is presented (Agathangelidis et al., 2019; Cohard et al., 2018; Dou et al., 2019; Hong et al., 2020; Shi et al., 2018). It notably represents the ratio of sensible heat fluxes (H) to latent heat fluxes (LE) during day hours where a positive incoming radiation is recorded, giving a deeper insight in the evapotranspiration and convection process. As shown in Fig. 14 the Bowen-ratio based on both simulated heat fluxes by TEB-Hydro and TEB-Veg follows the seasonal variations given by observations. However, comparing the two models with each other, TEB-Hydro overestimates much less the observed ones, except for the months of April and October.

6. Discussion

Based on the results, the different model performances of monthly-simulated latent heat fluxes and the Bowen-ratios can be explained by the model development of TEB-Hydro related to groundwater processes in the subsoil (deep drainage limitation and soil water drainage of the sewer network). As shown in Fig. 6, the comparison of TEB-Hydro and TEB-Veg simulated soil water content to observations highlights the strong impact of the newly introduced hydrological processes. Indeed, the TEB-Hydro configuration exacerbates the difficulties for ISBA to simulate weak soil water content during dry periods, while during wet periods, both configurations lead to almost the same values. Furthermore, the drainage of ground water by the sewer network may represent a significant proportion of the annual water budget, as about 20% were observed for the Pin Sec catchment and contributes to the availability of soil water for latent heat release. In order to take this into account in TEB-Hydro, the deep drainage was limited, leading to a strong moistening of the deep soil layers, especially during dry periods. However, as shown in Fig. 5, this effect is still visible in the 6^{th} soil layer close to the surface (equivalent soil depth of 35 cm). Such an excessive moistening, in turn, could explain the overestimation of latent heat fluxes compared to TEB-Veg. As a consequence, this model behaviour could lead to overestimate urban vegetation impacts on cooling effects and to underestimate urban landscape irrigation needs to maintain vegetation based NBSs performances (Daniel et al., 2018). Therefore, this outcome should question the actual C_{rech} value issued from model calibration, suggesting a modification of this actual process. As possible solutions, this parameter could be constantly changed to a lower limit and thus showing better performances in simulating both water and energy fluxes, essential to NBSs evaluation. Considering the results of the Bowen-ratio (Fig. 14), simulations are in favour of TEB-Hydro. They notably demonstrate that adding relevant urban hydrological processes to the model can improve heat flux simulations and the reproduction of observed trends and seasonal variations. This underlines the findings of Mitchell et al. (2008), who consider the coupling of both the water and energy balances to analyse the potential of urban space design based on greening.

Concerning the poor performance of TEB-Hydro in 2012 simulated latent heat fluxes, the incomplete dataset may be the cause. Indeed, for both years 2011 and 2012, the available data is limited (less than 25%) (Fig. 3 and Fig. 4). In addition, the 2012 dataset is not homogeneous as no data is recorded from September to December. As TEB-Hydro shows better skills during these winter months, TEB-Hydro's NSE for the simulated latent heat fluxes is lower than the TEB-Veg one.

Increasing latent heat fluxes, while the heat flux storage nearly stays the same during daytime (Fig. 12), has an impact on the energy budget. As a result, sensible heat fluxes seem to decrease with TEB-Hydro configuration. The model skill in simulating sensible heat fluxes is then improved, at both monthly and the 3-year period scales. This is also reflected by the monthly averaged Bowen-ratio for the 3-year period (Fig. 14). Such outcomes are important when analysing urban overheating and related heat stress in urban spaces during heat waves and urban heat island (UHI) phenomena. It could give insights in the regulation of ambient temperature and the cooling potential of urban greening during daytime and help adapting urban space design where needed (Emmanuel and Loconsole, 2015; Matthews et al., 2015). On the contrary, TEB-Hydro configuration does not improve sensible heat flux simulation during night-time. This is probably related to too high surface temperatures. However, without any observed data, this hypothesis cannot be confirmed. As stated by Norton et al. (2015), night-time temperatures in urban environments are essential for recovering from the thermal heat stress experienced during day time. Affecting human health and urban liveability, Kabisch et al. (2017) relate those issues to the multiple roles of NBSs facing urbanization-induced challenges. In this context, an overestimation of night-time sensible heat fluxes could thus overestimate UHI phenomena and, in turn, underestimate the thermal comfort related benefits of urban greening.

7. Conclusions

Nature-based solutions are supposed to mitigate urbanization effects, by reintroducing vegetation in cities. This offers, among other processes, evapotranspiration processes improving both urban water management and thermal comfort. Urban stakeholders thus need a systemic evaluation approach, for treating both water and energy issues in a coherent way. Therefore, a hydro-microclimate model (TEB-Hydro) was developed by improving the water budget of a well-known urban energy budget model (TEB-Veg). If the hydrological evaluation of TEB-Hydro had shown good skills in Stavropulos-Laffaille et al. (2018), the impact of the water budget modification in the subsoil on the energy budget had to be examined.

These water process developments in an urban surface energy model lead to simulating both detailed water and energy variables: discharge, soil water content, latent and sensible heat fluxes. Moreover, the surface type contribution for each of the heat and water fluxes is available. Thanks to an integral dataset of water and energy fluxes of the Pin Sec catchment, TEB-Hydro energy fluxes are evaluated, with regards to the new water budget. Based on the hydrological model calibration on total observed storm water sewer

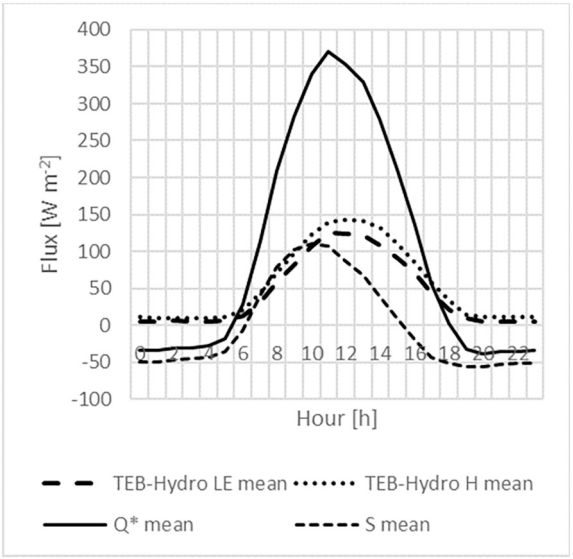

Fig. 12. Multi-year monthly averages of latent (LE), sensible (H) heat fluxes, net radiation (***Q****) and ground heat fluxes (S) simulated by TEB-Hydro.

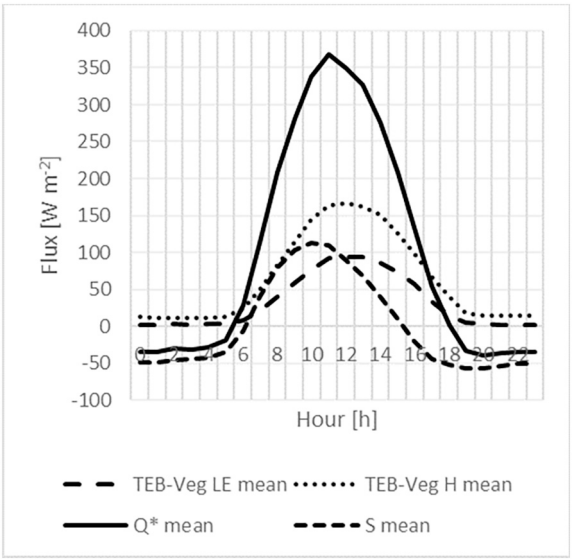

Fig. 13. Multi-year monthly averages of latent (LE), sensible (H) heat fluxes, net radiation (***Q****) and ground heat fluxes (S) simulated by TEB-Veg.

discharges by Stavropulos-Laffaille et al. (2018), the model shows also good results in simulating the energy budget: Indeed, the comparison between heat fluxes, simulated by TEB-Hydro and TEB-Veg over a 3-year period, highlights better scores for TEB-Hydro than for TEB-Veg. At a monthly scale, this result is still true for sensible heat fluxes, essential for analysing day-time human thermal comfort. However, excessive simulated sensible heat fluxes during night-time alters potential UHI analyses. Concerning latent heat fluxes, TEB-Hydro performs better than TEB-Veg during wet seasons, but not during dry seasons. This difficulty is linked to the limitation of deep drainage added to TEB-Hydro. The calibrated parameter, proposed by Stavropulos-Laffaille et al. (2018), is probably too high, excessively wetting soil even at a weak depth. This, in turn, could lead to overestimating the urban cooling potential of vegetation and to underestimate urban landscape irrigation needs during hot seasons.

The measurement of heat fluxes in urban areas can be questionable, depending on wind atmospheric conditions. Usually, a footprint method is used in order to identify the source zone contributing to measured heat fluxes. Based on wind direction observations, it allows to select only data for which the source zone covers the simulation domain. Such a method was tested. However, the resulting sample data, already initially strongly reduced to guarantee high quality data, was too small to allow a confident evaluation. Therefore, in order to confirm the results of this study, it should be continued over a longer simulation period, in order to increase available high quality observation data. Another urban catchment, under different climate conditions should also be studied.

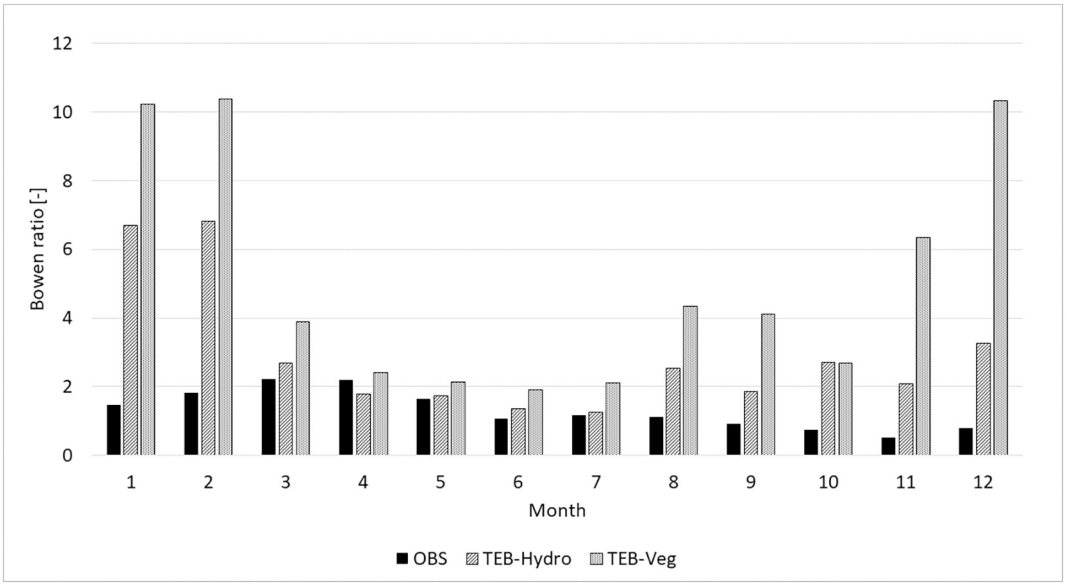

Fig. 14. Representation of the multy-year monthly averages of the Bowen ratio for observations (black), TEB-Hydro and TEB-Veg

Finally, the evaluation of TEB-Hydro and its comparison with TEB-Veg confirm the importance of an accurate simulation of soil water processes and soil-atmosphere water transfer in order to correctly simulate energy fluxes in urban areas. This finding is to highlight as nowadays vegetation is put forward to contribute to the urban microclimate (e.g. outdoor thermal comfort, UHI, etc.) and water management (storm water, water resources, water conservation planning, etc.). However, at the moment, only a few NBSs are available in the model (urban vegetation, green roofs and trees). Current developments are undergoing with the aim of proposing further solutions (swales, bio retention, porous pavements, etc.) to evaluate adaptation strategies based on urban green and blue infrastructures as well as to help building future, more sustainable cities.

Code and data availability

The surface modelling platform SURFEX is accessible on open source, where the codes of surface designs TEB and ISBA can be downloaded (http://www.cnrm-game-meteo.fr/surfex/, last access: 4 September 2018). This platform is regularly updated. For all further information or access to real-time code modifications, please follow the procedure in order to open the SVN account provided via the previous link. The routines modified with respect to the TEB-Hydro model SURFEX v7.3, as well as the run directories of the model experiments described in Stavropulos-Laffaille et al., 2018, may be retrieved via doi:https://doi.org/10.5281/zenodo.1218016. The Pin Sec catchment databases and the EC dataset are available upon request submitted to the authors.

Declaration of Competing Interest

The authors declare that they have no known competing financial interests or personal relationships that could have appeared to influence the work reported in this paper.

Acknowledgments

The authors would like to thank the *Nantes-Métropole* Metropolitan Government (Geographic Information Division) for providing the GIS data used herein. They thank also the anonymous reviewer for his pertinent remarks. Special thanks to Sophie Provost for proofreading.

References

Agathangelidis, I., Cartalis, C., Santamouris, M., 2019. Integrating urban form, function, and energy fluxes in a heat exposure indicator in view of intra-urban Heat Island assessment and climate change adaptation. Climate 7.

Bagga, I., 2012. Mesure et analyse des flux thermo-hydriques en zone hétérogène (SAP de l'IRSTV) (PhD Thesis). Ecole Centrale de Nantes.

Belhadj, N., Joannis, C., Raimbault, G., 1995. Modelling of rainfall induced infiltration into separate sewerage. Water Sci. Technol. 32, 161–168. https://doi.org/10.1016/0273-1223 (95)00551-W.

Berland, A., Shiflett, S.A., Shuster, W.D., Garmestani, A.S., Goddard, H.C., Herrmann, D.L., Hopton, M.E., 2017. The role of trees in urban stormwater management. Landsc. Urban Plan. 162, 167–177. https://doi.org/10.1016/j.landurbplan.2017.02.017.

Berthier, E., Andrieu, H., Creutin, J.D., 2004. The role of soil in the generation of urban runoff: development and evaluation of a 2D model. J. Hydrol. 299, 252–266. https://doi.org/10.1016/j.jhydrol.2004.08.008.

Berthier, E., Dupont, S., Mestayer, P.G., Andrieu, H., 2006. Comparison of two evapotranspiration schemes on a sub-urban site. J. Hydrol. 328, 635–646. https://doi.org/10.1016/j.jhydrol.2006.01.007.
Boone, A., Calvet, J.-C., Noilhan, J., 1999. Inclusion of a third soil layer in a land surface scheme using the force restore method. J. Appl. Meteorol. 38, 1611–1630. https://doi.org/10.1175/1520-0450(1999)038<1611:IOATSL>2.0.CO;2.
Coccolo, S., Kämpf, J., Mauree, D., Scartezzini, J.-L., 2018. Cooling potential of greening in the urban environment, a step further towards practice. Sustain. Cities Soc. 38, 543–559. https://doi.org/10.1016/j.scs.2018.01.019.
Cohard, J.-M., Rosant, J.-M., Rodriguez, F., Andrieu, H., Mestayer, P.G., Guillevic, P., 2018. Energy and water budgets of asphalt concrete pavement under simulated rain events. Urban Clim. 24, 675–691. https://doi.org/10.1016/j.uclim.2017.08.009.
Daniel, M., Lemonsu, A., Viguié, V., 2018. Role of watering practices in large-scale urban planning strategies to face the heat-wave risk in future climate. In: Urban Climate, ICUC9: The 9th International Conference on Urban Climate 23, pp. 287–308. https://doi.org/10.1016/j.uclim.2016.11.001.
de Munck, C.S., Lemonsu, A., Bouzouidja, R., Masson, V., Claverie, R., 2013. The GREENROOF module (v7.3) for modelling green roof hydrological and energetic performances within TEB. Geosci. Model Dev. 6, 1941–1960. https://doi.org/10.5194/gmd-6-1941-2013.
Decharme, B., Boone, A., Delire, C., Noilhan, J., 2011. Local evaluation of the interaction between soil biosphere atmosphere soil multilayer diffusion scheme using four pedotransfer functions. J. Geophys. Res.-Atmos. 116 https://doi.org/10.1029/2011JD016002.
DHI, 2012. MIKE SHE User Manual.
DiGiovanni-White, K., Montalto, F., Gaffin, S., 2018. A comparative analysis of micrometeorological determinants of evapotranspiration rates within a heterogeneous urban environment. J. Hydrol. 562, 223–243. https://doi.org/10.1016/j.jhydrol.2018.04.067.
Dou, J., Grimmond, S., Cheng, Z., Miao, S., Feng, D., Liao, M., 2019. Summertime surface energy balance fluxes at two Beijing sites. Int. J. Climatol. 39, 2793–2810. https://doi.org/10.1002/joc.5989.
Emmanuel, R., Loconsole, A., 2015. Green infrastructure as an adaptation approach to tackling urban overheating in the Glasgow Clyde Valley Region, UK. Landsc. Urban Plan. 138, 71–86. https://doi.org/10.1016/j.landurbplan.2015.02.012.
Fletcher, T.D., Andrieu, H., Hamel, P., 2013. Understanding, management and modelling of urban hydrology and its consequences for receiving waters: a state of the art. Adv. Water Resour. 51, 261–279. https://doi.org/10.1016/j.advwatres.2012.09.001.
Foken, T., Munger, J.W., Gockede, M., Mauder, M., Mahrt, L., Amiro, B.D., 2004. Post-field quality control. In: Handbook of Micro-meteorology: A Guide for Surface Flux Measurements. Kluwer Academic.
Fortuniak, K., Pawlak, W., Siedlecki, M., 2013. Integral turbulence statistics over a central European city centre. Bound.-Layer Meteorol. 257–276. https://doi.org/10.1007/s10546-012-9762-1.
Golden, H.E., Hoghooghi, N., 2018. Green infrastructure and its catchment-scale effects: an emerging science. WIREs Water 5, e1254. https://doi.org/10.1002/wat2.1254.
Grimmond, S., 2007. Urbanization and global environmental change: local effects of urban warming. Geogr. J. 173, 83–88. https://doi.org/10.1111/j.1475-4959.2007.232_3.x.
Grimmond, C.S.B., Oke, T.R., 1991. An evapotranspiration-interception model for urban areas. Water Resour. Res. 27, 1739–1755. https://doi.org/10.1029/91WR00557.
Grimmond, C.S.B., Blackett, M., Best, M.J., Barlow, J., Baik, J.-J., Belcher, S.E., Bohnenstengel, S.I., Calmet, I., Chen, F., Dandou, A., Fortuniak, K., Gouvea, M.L., Hamdi, R., Hendry, M., Kawai, T., Kawamoto, Y., Kondo, H., Krayenhoff, E.S., Lee, S.-H., Loridan, T., Martilli, A., Masson, V., Miao, S., Oleson, K., Pigeon, G., Porson, A., Ryu, Y.-H., Salamanca, F., Shashua-Bar, L., Steeneveld, G.-J., Tombrou, M., Voogt, J., Young, D., Zhang, N., 2010. The international urban energy balance models comparison project: first results from phase 1. J. Appl. Meteorol. Climatol. 49, 1268–1292. https://doi.org/10.1175/2010JAMC2354.1.
Grimmond, C.S.B., Blackett, M., Best, M.J., Baik, J.-J., Belcher, S.E., Beringer, J., Bohnenstengel, S.I., Calmet, I., Chen, F., Coutts, A., Dandou, A., Fortuniak, K., Gouvea, M.L., Hamdi, R., Hendry, M., Kanda, M., Kawai, T., Kawamoto, Y., Kondo, H., Krayenhoff, E.S., Lee, S.-H., Loridan, T., Martilli, A., Masson, V., Miao, S., Oleson, K., Ooka, R., Pigeon, G., Porson, A., Ryu, Y.-H., Salamanca, F., Steeneveld, G.J., Tombrou, M., Voogt, J.A., Young, D.T., Zhang, N., 2011. Initial results from Phase 2 of the international urban energy balance model comparison. Int. J. Climatol. 31, 244–272. https://doi.org/10.1002/joc.2227.
Gros, A., Bozonnet, E., Inard, C., Musy, M., 2016. Simulation tools to assess microclimate and building energy ? A case study on the design of a new district. Energy Build. 114, 112–122. https://doi.org/10.1016/j.enbuild.2015.06.032.
Gupta, H.V., Kling, H., Yilmaz, K.K., Martinez, G.F., 2009. Decomposition of the mean squared error and NSE performance criteria: implications for improving hydrological modelling. J. Hydrol. 377, 80–91. https://doi.org/10.1016/j.jhydrol.2009.08.003.
Hamel, P., Daly, E., Fletcher, T.D., 2013. Source-control stormwater management for mitigating the impacts of urbanisation on baseflow: a review. J. Hydrol. 485, 201–211. https://doi.org/10.1016/j.jhydrol.2013.01.001.
Hesslerová, P., Pokorný, J., Huryna, H., Seják, J., Jirka, V., 2021. The impacts of greenery on urban climate and the options for use of thermal data in urban areas. Prog. Plan. 100545 https://doi.org/10.1016/j.progress.2021.100545.
Hong, J.-W., Lee, S.-D., Lee, K., Hong, J., 2020. Seasonal variations in the surface energy and CO2 flux over a high-rise, high-population, residential urban area in the East Asian monsoon region. Int. J. Climatol. 40, 4384–4407. https://doi.org/10.1002/joc.6463.
Ibrom, A., Dellwik, E., Flyvbjerg, H., Jensen, N.O., Pilegaard, K., 2007. Strong low-pass filtering effects on water vapour flux measurements with closed-path eddy correlation systems. Agric. For. Meteorol. 147, 140–156. https://doi.org/10.1016/j.agrformet.2007.07.007.
Kabisch, N., van den Bosch, M., Lafortezza, R., 2017. The health benefits of nature-based solutions to urbanization challenges for children and the elderly – a systematic review. Environ. Res. 159, 362–373. https://doi.org/10.1016/j.envres.2017.08.004.
Krayenhoff, E., Christen, A., Martilli, A., Oke, T., 2014. A multi-layer radiation model for urban neighbourhoods with trees. Bound.-Layer Meteorol. 139–178. https://doi.org/10.1007/s10546-013-9883-1.
Krayenhoff, E., Santiago, J.-L., Martilli, A., Christen, A., Oke, T., 2015. Parametrization of drag and turbulence for urban neighbourhoods with trees. Bound.-Layer Meteorol. https://doi.org/10.1007/s10546-015-0028-6.
Krayenhoff, E.S., Jiang, T., Christen, A., Martilli, A., Oke, T.R., Bailey, B.N., Nazarian, N., Voogt, J.A., Giometto, M.G., Stastny, A., Crawford, B.R., 2020. A multi-layer urban canopy meteorological model with trees (BEP-Tree): street tree impacts on pedestrian-level climate. Urban Clim. 32, 100590. https://doi.org/10.1016/j.uclim.2020.100590.
Lafortezza, R., Chen, J., van den Bosch, C.K., Randrup, T.B., 2018. Nature-based solutions for resilient landscapes and cities. Environ. Res. 165, 431–441. https://doi.org/10.1016/j.envres.2017.11.038.
Lee, S.-H., Park, S.-U., 2008. A vegetated urban canopy model for meteorological and environmental modelling. In: Boundary - Layer Meteorology, 126, pp. 73–102.
Lemonsu, A., Masson, V., Berthier, E., 2007. Improvement of the hydrological component of an urban soil-vegetation-atmosphere-transfer model. Hydrol. Process. 21, 2100–2111. https://doi.org/10.1002/hyp.6373.
Lemonsu, A., Masson, V., Shashua-Bar, L., Erell, E., Pearlmutter, D., 2012. Inclusion of vegetation in the Town Energy Balance model for modelling urban green areas. Geosci. Model Dev. 5, 1377–1393. https://doi.org/10.5194/gmd-5-1377-2012.
Litvak, E., Manago, K.F., Hogue, T.S., Pataki, D.E., 2017. Evapotranspiration of urban landscapes in Los Angeles, California at the municipal scale. Water Resour. Res. 53, 4236–4252. https://doi.org/10.1002/2016WR020254.
Liu, X., Li, X.-X., Harshan, S., Roth, M., Velasco, E., 2017. Evaluation of an urban canopy model in a tropical city: the role of tree evapotranspiration. Environ. Res. Lett. 12, 094008 https://doi.org/10.1088/1748-9326/aa7ee7.
Locatelli, L., Mark, O., Mikkelsen, P.S., Arnbjerg-Nielsen, K., Deletic, A., Roldin, M., Binning, P.J., 2017. Hydrologic impact of urbanization with extensive stormwater infiltration. J. Hydrol. 544, 524–537. https://doi.org/10.1016/j.jhydrol.2016.11.030.
Masson, V., 2000. A physically-based scheme for the urban energy budget in atmospheric models. Bound.-Layer Meteorol. 94, 357–397. https://doi.org/10.1023/A:1002463829265.
Matthews, T., Lo, A.Y., Byrne, J.A., 2015. Reconceptualizing green infrastructure for climate change adaptation: barriers to adoption and drivers for uptake by spatial planners. Landsc. Urban Plan. 138, 155–163. https://doi.org/10.1016/j.landurbplan.2015.02.010.

Mestayer, P., Chancibault, K., Lebouc, L., Letellier, L., Mosini, M.-L., Rodriguez, F., Rouaud, M., Bagga, I., Calmet, I., Fontanilles, G., Gaudin, D., Ho Lee, J., Piquet, T., Rosant, J.-M., Sabre, M., Tétard, Y., Brut, A., Selves, J.-L., Solignac, P.-A., Dayau, S., Irvine, M., Lagouarde, J.-P., Kassouk, Z., Launeau, P., Connan, O., Defenouillère, P., Goriaux, M., Hébert, D., Letellier, B., Maro, D., Najjar, G., Nerry, F., Quentin, C., Biron, R., Cohard, J.-M., Galvez, J., Klein, P., 2011. FluxSAP 2010 experimental campaign over an heterogeneous urban zone, part 1: heat and vapour flux assessement. In: Conference on Harmonisation within Atmospheric Dispersion Modelling for Regulatory Purposes. Presented at the 14th Conference on Harmonisation within Atmospheric Dispersion Modelling for Regulatory Purposes, Greece, pp. 433–437.

Mitchell, V.G., Cleugh, H.A., Grimmond, C.S.B., Xu, J., 2008. Linking urban water balance and energy balance models to analyse urban design options. Hydrol. Process. 22, 2891–2900. https://doi.org/10.1002/hyp.6868.

Moriasi, D., Arnold, J., Van Liew, M., Bingner, R., Harmel, R., Veith, T., 2007. Model evaluation guidelines for systematic quantification of accuracy in watershed simulations. Trans. ASABE 50, 885–900. https://doi.org/10.13031/2013.23153.

Nice, K.A., Coutts, A.M., Tapper, N.J., 2018. Development of the VTUF-3D v1.0 urban micro-climate model to support assessment of urban vegetation influences on human thermal comfort. Urban Clim. 24, 1052–1076. https://doi.org/10.1016/j.uclim.2017.12.008.

Norton, B.A., Coutts, A.M., Livesley, S.J., Harris, R.J., Hunter, A.M., Williams, N.S.G., 2015. Planning for cooler cities: a framework to prioritise green infrastructure to mitigate high temperatures in urban landscapes. Landsc. Urban Plan. 134, 127–138. https://doi.org/10.1016/j.landurbplan.2014.10.018.

O'Driscoll, M., Clinton, S., Jefferson, A., Manda, A., McMillan, S., 2010. Urbanization effects on watershed hydrology and in-stream processes in the Southern United States. Water 2, 605. https://doi.org/10.3390/w2030605.

Oke, T.R., 1987. Boundary Layer Climates, 2nd ed. Routledge.

Redon, E.C., Lemonsu, A., Masson, V., Morille, B., Musy, M., 2017. Implementation of street trees within the solar radiative exchange parameterization of TEB in SURFEX v8.0. Geosci. Model Dev. 10, 385–411. https://doi.org/10.5194/gmd-10-385-2017.

Redon, E., Lemonsu, A., Masson, V., 2020. An urban trees parameterization for modeling microclimatic variables and thermal comfort conditions at street level with the Town Energy Balance model (TEB-SURFEX v8.0). Geosci. Model Dev. 13, 385–399. https://doi.org/10.5194/gmd-13-385-2020.

Rodriguez, F., Morena, F., Andrieu, H., 2005. Development of a distributed hydrological model based on urban databanks - production processes of URBS. Water Sci. Technol. 52, 241–248.

Rodriguez, F., Le Delliou, A.-L., Andrieu, H., Gironás, J., 2020. Groundwater contribution to sewer network baseflow in an urban catchment-case study of pin sec catchment, Nantes, France. Water 12, 689. https://doi.org/10.3390/w12030689.

Ryu, Y.-H., Bou-Zeid, E., Wang, Z.-H., Smith, J.A., 2016. Realistic representation of trees in an urban canopy model. Bound.-Layer Meteorol. 159, 193–220. https://doi.org/10.1007/s10546-015-0120-y.

Shi, Y., Lau, K.K.-L., Ren, C., Ng, E., 2018. Evaluating the local climate zone classification in high-density heterogeneous urban environment using mobile measurement. Urban Clim. 25, 167–186. https://doi.org/10.1016/j.uclim.2018.07.001.

Stavropulos-Laffaille, X., Chancibault, K., Brun, J.-M., Lemonsu, A., Masson, V., Boon, A., Andrieu, H., 2018. Improvements to the hydrological processes of the Town Energy Balance model (TEB-Veg, SURFEX v7.3) for urban modelling and impact assessment. Geosci. Model Dev. 11, 4175–4194. https://doi.org/10.5194/gmd-11-4175-2018.

Sutherland, R.C., 2000. Methods for estimating the effective impervious area of urban watersheds. Pract. Watershed Protect. 32, 193–195.